Current Applied Physics 20 (2020) 746–750

Contents lists available at ScienceDirect

Current Applied Physics

journal homepage: www.elsevier.com/locate/cap

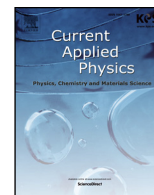

Dynamic analysis of non-linear wake-up behavior in $Hf_{0.7}Zr_{0.3}O_2$ thin film

J.C. Choi[a], M.S. Song[a], K. Lee[a], K. Park[b,c], J. Park[b,c], H. Lee[d], J.H. Lee[d], S.C. Chae[a,*]

[a] *Department of Physics Education, Seoul National University, Seoul, 08826, Republic of Korea*
[b] *School of Chemical and Biological Engineering, Institute of Chemical Processes, Seoul National University, Seoul, 08826, Republic of Korea*
[c] *Center for Nanoparticle Research, Institute for Basic Science (IBS), Seoul National University, Seoul, 08826, Republic of Korea*
[d] *Department of Energy Engineering, School of Energy and Chemical Engineering, Ulsan National Institute of Science and Technology (UNIST), Ulsan, 44919, Republic of Korea*

ARTICLE INFO

Keywords:
$Hf_{1-x}Zr_xO_2$
Ferroelectricity
Wake-up effect

ABSTRACT

We report on the nonlinear wake-up behavior against the external electric field cycling in the ferroelectric $Hf_{0.7}Zr_{0.3}O_2$ thin film. Two distinct scaling regimes during the increase of the remnant polarization with different activation energies were observed in TiN/$Hf_{0.7}Zr_{0.3}O_2$/TiN cells. The transmission electron microscopy revealed the structural phase transition from the monoclinic structure to the orthorhombic structure of the $Hf_{0.7}Zr_{0.3}O_2$ film after the wake-up behavior. During the phase change, as the remnant polarization enhanced, the dielectric constant of the $Hf_{0.7}Zr_{0.3}O_2$ film increased with the external field cycling. The temperature dependence of the wake-up behavior revealed that each estimated activation energies for the early and later enhancement of the remnant polarization are 1.12 eV and 0.73 eV, respectively. First principle calculations show that the oxygen vacancies can reduce the activation energy barrier for the structural phase transition.

1. Introduction

HfO_2-based ferroelectric thin films have attracted attention for the application of non-volatile ferroelectric memory devices [1]. The robust ferroelectricity with compatibility on the current complementary metal oxide semiconductor device process enables the practical non-volatile device application using HfO_2 thin film [2]. Since the discovery of ferroelectricity in polycrystalline HfO_2 film [1], the characterization of ferroelectricity in terms of stability as a memory device has reported high endurance with 10^8–10^{10} switching cycles and retention properties up to 10^3 h at 125 °C [3,4]. In addition, besides practical application structures like ferroelectric tunnel junctions or ferroelectric field-effect transistor [5–7], the negative capacitance has opened an avenue for the next generation of memory applications using ferroelectric HfO_2 [8,9].

A variation of the remnant polarization during the external field cycling has been investigated severely in light of the elucidation of the uncertainty of the non-volatile memory. The enhancement of the remnant polarization value known as a wake-up behavior was observed depending on the deposition conditions [10] and the type of electrode material [11]. This wake-up behavior was often accompanied by the change of hysteresis from antiferroelectric to ferroelectric depending on dopants (Si, Zr, La) [10]. The variation of the remnant polarization owing to the wake-up behavior can be an obstacle to apply ferroelectric HfO_2 thin films to non-volatile memory devices. Prior to the practical application, a clear understanding of the mechanism for the wake-up behavior is required [12].

Various mechanisms have been proposed for the wake-up behavior, such as the redox reaction on the interfaces, a pinning-depinning effect of the ferroelectric domains by defects, and structural phase transitions [11,13]. The wake-up behavior with different metal-ferroelectric interfaces was investigated in terms of the density of oxygen vacancies which correlate with the stability of the orthorhombic structure [11]. The redistribution of oxygen vacancies and charge trapping-detrapping were proposed through the harmonic analysis of the evolution of the hysteresis loop during the external field cycling [14,15]. In addition, the field-induced structural phase transition has also been considered for the origin of the wake-up behavior [16]. The scanning transmission electron microscopy revealed a tetragonal-to-orthorhombic structural phase transition and a monoclinic-to-orthorhombic phase transition at the interface and the bulk, respectively [17]. Furthermore, the increase of a cubic phase and the suppression of the monoclinic phase were also reported to stabilize the orthorhombic phase during the external field cycling [18]. These mechanisms were proposed with the theoretical argument for ionic contribution or ex-situ analysis of structural deformation after the external field cycling. Therefore, the detailed dynamic analysis of the remnant polarization enhancement will enlarge our understanding of the underlying mechanism for the wake-up

* Corresponding author.
E-mail address: scchae@snu.ac.kr (S.C. Chae).

https://doi.org/10.1016/j.cap.2020.03.012
Received 27 November 2019; Received in revised form 4 March 2020; Accepted 11 March 2020
Available online 13 March 2020
1567-1739/ © 2020 Korean Physical Society. Published by Elsevier B.V. All rights reserved.

behavior.

In this letter, we investigated the subsequent external field cycling dependence of the wake-up behavior of the ferroelectric $Hf_{0.7}Zr_{0.3}O_2$ film. After the wake-up behavior, the direct phase transition was investigated by the high-resolution transmission electron microscopy (HRTEM). The capacitance-voltage (C–V) measurement exhibited the nonlinear increase of the permittivity with the wake-up behavior. The temperature dependence of the wake-up behavior was analyzed by the Johnson-Mehl-Avrami (JMA) model which has been used to understand the various transition in terms of the nucleation and grain growth [19].

2. Material and methods

We fabricated the ferroelectric $Hf_{0.7}Zr_{0.3}O_2$ film by using the atomic layer deposition (ALD) method. For the ALD growth, we used tetrakis (ethylmethylamido) hafnium (TEMAH), tetrakis (ethylmethylamido) zirconium (TEMAZ) and ozone. 10-nm-thick $Hf_{0.7}Zr_{0.3}O_2$ films were grown at 280 °C. The titanium nitride (TiN) bottom and top electrodes were deposited by DC sputtering. The polarization-voltage (P–V) hysteresis was performed after each of the finite numbers of the external bias sweep with a semiconductor parameter analyzer (Model 4200-SCS, Keithley) and ferroelectric tester (TF Analyzer 3000, aixACCT). The cation composition and crystallographic phases of the films were examined using a transmission electron microscopy (JEOL ARM 200F). The C–V measurements were performed by using an impedance analyzer (Model E4990A, Keysight). For the theoretical estimation of the energy difference between the monoclinic structure and the orthorhombic structure, we conducted first-principle calculations based on the density functional theory using the Vienna Ab initio calculation package code (VASP Software GmbH, Vienna, Austria).

3. Results and discussions

The ferroelectric $Hf_{0.7}Zr_{0.3}O_2$ film exhibited the typical wake-up behavior under the subsequent external field cycling. Fig. 1(a) shows the P–V curves of the ferroelectric $Hf_{0.7}Zr_{0.3}O_2$ film for the pristine specimen and specimens after the external field cycling of 50 000, 100 000 and 300 000 times, respectively. P–V hysteresis curves using a positive-up-negative-down (PUND) method were measured after each of 10 000 cycles of the external field cycling with a frequency of 10 kHz at 7 V [20]. Although ferroelectricity was not found in the pristine sample, the external field cycling enabled the evolution of ferroelectricity with $2P_r$ ~60 μC/cm². The dashed hysteresis curves demonstrate the systematic change of ferroelectricity before 50 000 cycles. Fig. 1(b) shows that the coercivity decreased during 50 000 external field cycling and the remnant polarization value increased continuously. On the other hand, the rest wake-up behavior exhibited only the increase of the remnant polarization value without the additional change of the coercivity. This difference between the early and later wake-up behavior can be considered with the reduced depolarization field near the metal-HfO_2 interfaces. HfO_2 based ferroelectric thin film has a non-ferroelectric monoclinic phase with oxygen vacancies near the metal-HfO_2 interfaces [11,21]. As the oxygen vacancies tend to stabilize the orthorhombic phase, the phase transition from the non-ferroelectric monoclinic phase to the ferroelectric orthorhombic phase occurs during the early wake-up behavior [17]. Even though the bulk region also can have the phase transition, the effective electric field engaged to the whole film won't change because the ferroelectric phase and non-ferroelectric phase are connected in parallel effectively [22]. Therefore, the decrease of the coercivity was observed during the initial wake-up behavior and the rest wake-up behavior shows polarization enhancement without the change of the coercivity.

The transmission electron microscopy manifested that the structural phase transition from the monoclinic to the orthorhombic phase was accompanied by the wake-up behavior. Figs. 1(c) and (d) show fast Fourier transform images of the HRTEM results of the pristine and

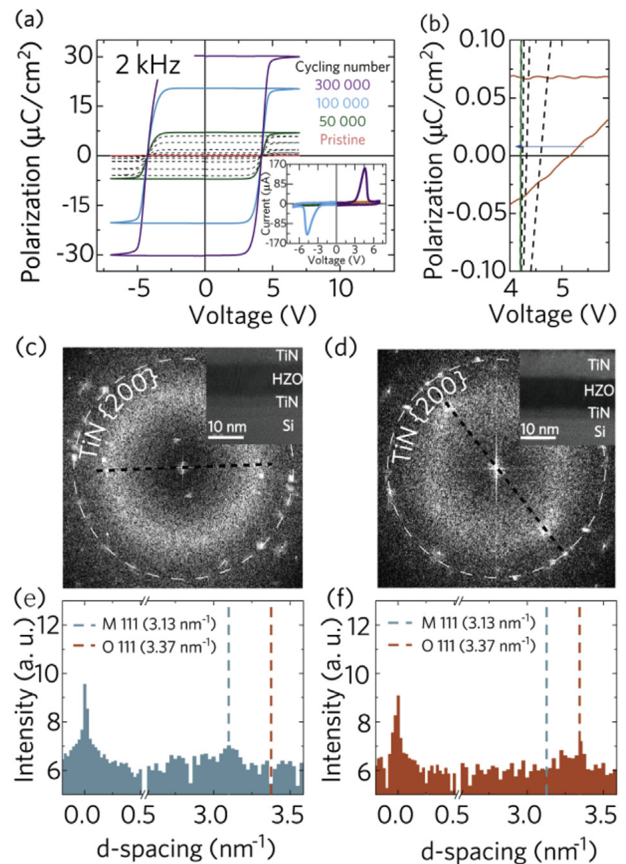

Fig. 1. (a) The hysteresis loops: pristine, 50 000 cycled, 100 000 cycled, 300 000 cycled woken-up specimens, respectively. The inset shows the I–V curve of the fully woken-up $Hf_{0.7}Zr_{0.3}O_2$ film. (b) The reduction of the coercivity of the hysteresis loops from pristine to 40 000 cycled wake-up. Diffraction patterns of fast Fourier transform images from (c) the pristine sample and (d) 300 000 cycled wake-up sample, respectively. The insets show the HRTEM image. (e) The intensity line profile of the black dashed line of Fig. 1(c). (f) The intensity line profile of the black dashed line of Fig. 1(d).

woken-up TiN/HZO/TiN/Si specimen shown in the inset, respectively. The diffraction patterns from polycrystalline TiN {200} layers were used for calibration. The strong diffraction pattern of (111) plane of the monoclinic phase in the pristine specimen was observed with d-spacing of 0.3195 nm noted with a black dashed line in Fig. 1(c). On the other hand, (111) plane of the orthorhombic phase diffraction pattern with d-spacing of 0.2967 nm noted with a black dashed line in Fig. 1(d) emerged with vanishing of the monoclinic diffraction pattern in the woken-up specimen. For clarity, Figs. 1(e) and (f) show the intensity line profile of the black dashed line in Figs. 1(c) and (d), respectively. Considered with the peak positions in the line profile, the diffraction patterns of the pristine and woken-up specimen demonstrate the clear structural change from the monoclinic structure to the orthorhombic structure after the wake-up behavior.

The evolution of the permittivity during the external field cycling was coincident with the enhancement of the remnant polarization. Fig. 2(a) shows the C–V curves with a small ac voltage of 10 kHz and 200 mV amplitude after each of 10 000 cycles of the external field cycling up to 200 000 cycles. Solid orange, red, green, blue, and purple lines represent the pristine and cycled specimens after 50 000, 100 000, 150 000 and 200 000, respectively. As the number of the external field cycling increased, the minimum value of the permittivity of each C–V measurement increased continuously from 17 to 19. The permittivity of the monoclinic phase and the orthorhombic, tetragonal phases are known to be 16–20 and 27–35, 28–70, respectively [23]. Even though

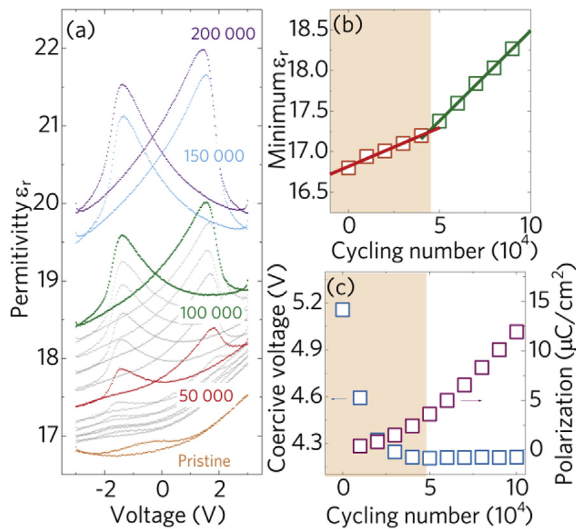

Fig. 2. (a) The C–V curves of the $Hf_{0.7}Zr_{0.3}O_2$ film. (b) The evolution of the minimum relative permittivity ε_r. (c) The coercivity (left side) and the remnant polarization (right side) as a function of a number of switching cycles.

the permittivity during the wake-up behavior is slightly less than the value of the orthorhombic phase, the increase of the permittivity can imply that the change from the monoclinic phase to the orthorhombic phase was accompanied by the wake-up behavior [24].

The wake-up behavior can be clearly distinguished into two different regimes during the external field cycling. To understand the evolution of the wake-up behavior, the permittivity and the coercivity were compared after every 10 000 cycles of the external field cycling. Fig. 2(b) shows the minimum value of the permittivity with the external field cycling extracted from Fig. 2(a). From the pristine to 50 000 cycled specimens, the minimum value of the permittivity increases by 2.4% from 16.8 to 17.2. In contrast, the minimum value of the permittivity from 50 000 to 100 000 cycled specimens increased by 5.8% from 17.3 to 18.3, almost two times larger than previous enhancement. Fig. 2(c) shows the evolution of the coercivity and remnant polarization with the external field cycling. The decrease of variation of the coercivity above 50 000 cycles was coincident with the change of the permittivity with different slopes. Note that the coercivity difference between the P–V and C–V measurements can be attributed to the frequency dependence of ferroelectric coercivity [25,26]. The P–V and C–V measurements were measured at 2 kHz and DC bias, respectively. The correspondence between the change in the permittivity and the variation of the coercivity evokes that the wake-up behavior can be attributed to the structural change.

Each enhancement of the remnant polarization in the two regimes follows the typical growth behavior by the nucleation and the expansion of the grain. Fig. 3(a) shows the external field cycling dependence of the remnant polarization under varying temperatures between 290 K and 320 K. The enhancement of the remnant polarization during the wake-up behavior became faster if the measurement temperature increased. The temperature dependence of the enhancement of the remnant polarization resembles the conventional growth behavior observed in the crystallization of amorphous materials, ferromagnetic and ferroelectric grain growth [27–29]. Most aforementioned cases can be described by the nucleation of the transformation and domain wall growth supposed by the JMA model [19].

The saturation behavior of the remnant polarization during the wake-up behavior demonstrated that the increase of the remnant polarization follows the JMA model. Using the JMA model, we predicted the amount of the enhanced remnant polarization phase as a function of N/f:

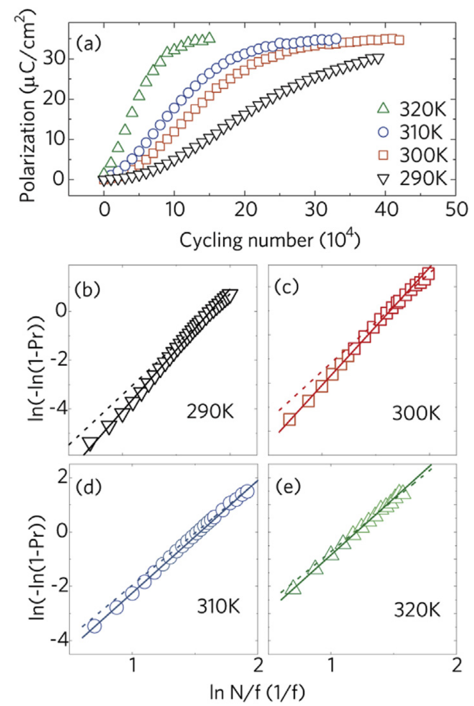

Fig. 3. (a) The evolution of the remnant polarization as a function of the number of the external field cycling and the JMA model fitting at the temperature of (b) 290 K, (c) 300 K, (d) 310 K, (e) 320 K, respectively.

$$P_r = 1 - \exp\left(-K\left(\frac{N}{f}\right)^m\right) \tag{1}$$

with

$$K(T) = K_o \exp\left(\frac{E_a}{k_B T}\right) \tag{2}$$

where N, f, m, K, E_a, T, and k_B are the external field cycling number, measurement frequency, the Avrami coefficient, an effective rate constant, the activation energy, temperature, and the Boltzmann constant, respectively. In order to compare the enhancement of the remnant polarization with respect to the JMA model, the JMA plot, i.e., ln (-ln (1-P_r)) vs ln N/f was obtained as shown in Figs. 3(b)-3(e). The experimental results showed two different scaling regions with different slopes for linear fits as depicted with the solid and dashed lines, respectively. As the measurement temperature increased, the difference between the slopes of linear fits decreased as shown in Figs. 3(b)-3(e). Fig. 4(a) shows the Arrhenius plots with two activation energies of 1.12 eV and 0.73 eV extracted from the slopes of the line fit in Figs. 3(b)-3(e). The different linearity indicates that the mechanism for the wake-up behavior was altered simultaneously during the external field cycling with a decrease of the activation energy.

The migration and redistribution of oxygen vacancies into the bulk region have been considered as a prominent origin for the wake-up behavior with the structural change from the monoclinic phase to the orthorhombic phase [17]. The migration of oxygen vacancies was reported to be essential for the ferroelectric structural phase transition of HfO_2 [15]. The activation energies of migration of oxygen vacancies in HfO_2 are known to be from 0.76 eV to 1.2 eV depending on the oxidation states [30]. Also experimentally, the activation energies for the oxygen vacancies are known to be from 1.01 eV to 1.03 eV depending on the doping concentration [31]. Taking into account the estimated activation energy in Fig. 4(a), oxygen vacancies may occur and the migration and redistribution of oxygen vacancies may alter the activation energy of phase transitions [11].

DFT calculations on the influence of oxygen vacancies on the phase

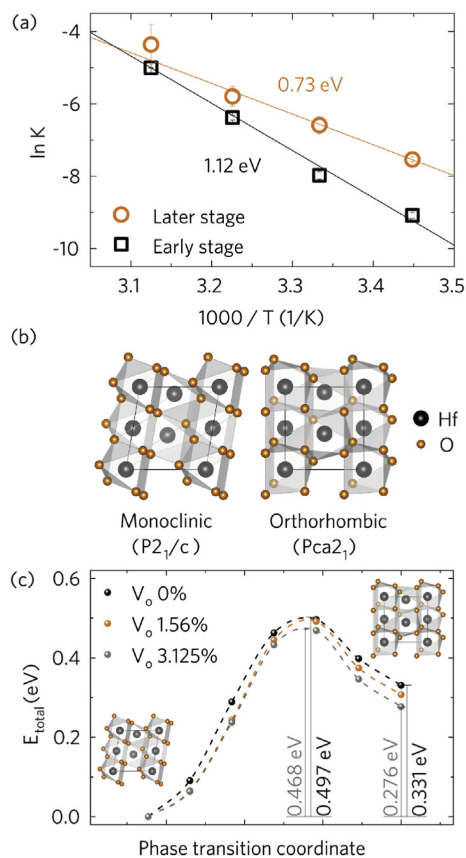

Fig. 4. (a) Arrhenius plots for the evolution of the remnant polarization with the activation energy of 1.12 eV and 0.73eV, respectively. Early and later stages were determined by the different linear enhancement of the electrical characteristics against the external field cycling. Data points were extracted from Figs. 3(b)–(e). (b) Schematic diagram of the crystal structure of the monoclinic and orthorhombic HfO_2. (c) Calculated activation energy barrier through the monoclinic to the orthorhombic phase transition using the LDA-DFT method.

transition from the monoclinic phase to the orthorhombic phase of bulk HfO_2 was carried out to understand the variation of activation energy with respect to the external field cycling. Fig. 4(b) shows the schematic diagram of the crystal structure of the monoclinic and the orthorhombic HfO_2 in the simulations. Fig. 4(c) shows the activation energy barrier from the monoclinic phase to the orthorhombic phase without oxygen vacancies defect and with oxygen vacancies of 1.56% and 3.125%. The activation energy barrier reduced 6% from 0.497 eV to 0.468 eV. After the transition, the total energy of the orthorhombic phase reduced 19% from 0.331 eV to 0.276 eV. The stabilization of the orthorhombic phase by oxygen vacancies is consistent with previous reports [11]. DFT calculations showed that oxygen vacancies stabilized the orthorhombic phase, and also reduce the activation energy barrier from the monoclinic to the orthorhombic phase. However, the activation energies of experimental measurement and theoretical calculation showed quite different values. In the DFT calculations, we calculated the bulk system, not the film, which might underestimate the activation energy. First, DFT could under/overestimate the bonding strength between Hf and O compared to experimental values. The estimated bonding energy, which could be weaker than the actual bonding energy, reduces the transition state energy and energy barrier. Second, extrinsic factors such as screening effect, strain, and defects could affect the effective field engaged on the HfO_2 film, the transition state energy by altering the real atomic structure, or local field near trap sites experimentally [32,33]. Since we assumed a bulk system, the total energy of the orthorhombic phase was calculated higher than the monoclinic phase. However, it has been reported that the total energy of the orthorhombic phase can be lower than the monoclinic phase with high compressive strain in the film [34]. The discrepancy between the experimental value and theoretical calculation can be moderated by the detailed chemical and local structure analysis.

4. Conclusion

In conclusion, we have demonstrated the wake-up behavior of the $Hf_{0.7}Zr_{0.3}O_2$ film. The HRTEM diffraction patterns implied the phase transition from the monoclinic phase to the orthorhombic phase during the wake-up behavior. The C–V measurement results demonstrated the nonlinear phase transition from the non-ferroelectric low permittivity phase to the relatively ferroelectric high permittivity phase during the wake-up behavior. The activation energies with the nonlinear wake-up behavior were extracted from JMA model. The DFT calculations revealed that oxygen vacancies can induce nonlinearity during the wake-up behavior. Our results provide insight into the mechanism of the wake-up behavior in hafnia based ferroelectric thin films.

Declaration of competing interest

The authors declare that they have no known competing financial interests or personal relationships that could have appeared to influence the work reported in this paper.

Acknowledgments

This work was supported MOTIE (Ministry of Trade, Industry & Energy) (no. 10080657) and KRSC (Korea Semiconductor Research Consortium) support program for the development of future semiconductor devices. Part of this study was performed using facilities at the IBS Center for Correlated Electron Systems, Seoul National University. J.H.L and H.J.L at UNIST were supported by Creative Materials Discovery Program (2017M3D1A1040828).

References

[1] T.S. Böscke, J. Müller, D. Bräuhaus, U. Schröder, U. Böttger, Ferroelectricity in hafnium oxide thin films, Appl. Phys. Lett. 99 (2011) 102903, , https://doi.org/10.1063/1.3634052.
[2] J. Müller, P. Polakowski, S. Mueller, T. Mikolajick, Ferroelectric hafnium oxide based materials and devices: assessment of current status and future prospects, ECS J. Solid State Sci. Technol. 4 (2015) N30–N35, https://doi.org/10.1149/2.0081505jss.
[3] J. Müller, T.S. Böscke, S. Müller, E. Yurchuk, P. Polakowski, J. Paul, D. Martin, T. Schenk, K. Khullar, A. Kersch, W. Weinreich, S. Riedel, K. Seidel, A. Kumar, T.M. Arruda, S.V. Kalinin, T. Schlösser, R. Boschke, R.v. Bentum, U. Schröder, T. Mikolajick, Ferroelectric hafnium oxide: a CMOS-compatible and highly scalable approach to future ferroelectric memories, IEEE International Electron Devices Meeting, 2013, 2013, https://doi.org/10.1109/IEDM.2013.6724605 10.8.1-10.8.4.
[4] K. Lee, T.Y. Lee, S.M. Yang, D.H. Lee, J. Park, S.C. Chae, Ferroelectricity in epitaxial Y-doped HfO_2 thin film integrated on Si substrate, Appl. Phys. Lett. 112 (2018) 202901, , https://doi.org/10.1063/1.5020688.
[5] H.Y. Yoong, H. Wu, J. Zhao, H. Wang, R. Guo, J. Xiao, B. Zhang, P. Yang, S.J. Pennycook, N. Deng, X. Yan, J. Chen, Epitaxial ferroelectric $Hf_{0.5}Zr_{0.5}O_2$ thin films and their implementations in memristors for brain-inspired computing, Adv. Funct. Mater. 28 (2018) 1806037, , https://doi.org/10.1002/adfm.201806037.
[6] S. Fujii, M. Saitoh, Chapter 10.3 - ferroelectric tunnel junction, in: U. Schroeder, C.S. Hwang, H. Funakubo (Eds.), Ferroelectricity in Doped Hafnium Oxide: Materials, Properties and Devices, Woodhead Publishing, Amsterdam, 2019, p. 437.
[7] M. Yamaguchi, S. Fujii, Y. Kamimuta, S. Kabuyanagi, T. Ino, Y. Nakasaki, R. Takaishi, R. Ichihara, M. Saitoh, Impact of specific failure mechanisms on endurance improvement for HfO2-based ferroelectric tunnel junction memory, IEEE International Reliability Physics Symposium (IRPS), IEEE International, 2018, , https://doi.org/10.1109/IRPS.2018.8353633 6D.2-1-6D.2-6.
[8] M. Hoffmann, M. Pešić, K. Chatterjee, A.I. Khan, S. Salahuddin, S. Slesazeck, U. Schroeder, T. Mikolajick, Direct observation of negative capacitance in polycrystalline ferroelectric HfO_2, Adv. Funct. Mater. 26 (2016) 8643–8649, https://doi.org/10.1002/adfm.201602869.
[9] K. Lee, H.-J. Lee, T.Y. Lee, H.H. Lim, M.S. Song, H.K. Yoo, D.I. Suh, J.G. Lee, Z. Zhu, A. Yoon, M.R. MacDonald, X. Lei, K. Park, J. Park, J.H. Lee, S.C. Chae, Stable subloop behavior in ferroelectric Si-doped HfO_2, ACS Appl. Mater. Interfaces 11 (2019) 38929–38936, https://doi.org/10.1021/acsami.9b12878.
[10] M.H. Park, Y.H. Lee, H.J. Kim, Y.J. Kim, T. Moon, K.D. Kim, J. Müller, A. Kersch,

U. Schroeder, T. Mikolajick, C.S. Hwang, Ferroelectricity and antiferroelectricity of doped thin HfO_2-based films, Adv. Mater. 27 (2015) 1811–1831, https://doi.org/10.1002/adma.201404531.

[11] M. Hoffmann, U. Schroeder, T. Schenk, T. Shimizu, H. Funakubo, O. Sakata, D. Pohl, M. Drescher, C. Adelmann, R. Materlik, A. Kersch, T. Mikolajick, Stabilizing the ferroelectric phase in doped hafnium oxide, Appl. Phys. Lett. 118 (2015) 072006, , https://doi.org/10.1063/1.4927805.

[12] G.R. Fox, R. Bailey, W.B. Kraus, F. Chu, S. Sun, T. Davenport, The current status of FeRAM, in: H. Ishiwara, M. Okuyama, Y. Arimoto (Eds.), Ferroelectric Random Access Memories: Fundamentals and Applications, Berlin, 2004, p. 139.

[13] T. Schenk, E. Yurchuk, S. Mueller, U. Schroeder, S. Starschich, U. Böttger, T. Mikolajick, About the deformation of ferroelectric hystereses, Appl. Phys. Rev. 1 (2014) 041103, , https://doi.org/10.1063/1.4902396.

[14] T. Schenk, U. Schroeder, M. Pešić, M. Popovici, Y.V. Pershin, T. Mikolajick, Electric field cycling behavior of ferroelectric hafnium oxide, ACS Appl. Mater. Interfaces 6 (2014) 19744–19751, https://doi.org/10.1021/am504837r.

[15] M. Pešić, F.P.G. Fengler, L. Larcher, A. Padovani, T. Schenk, E.D. Grimley, X. Sang, J.M. LeBeau, S. Slesazeck, U. Schroeder, T. Mikolajick, Physical mechanisms behind the field-cycling behavior of HfO_2-based ferroelectric capacitors, Adv. Funct. Mater. 26 (2016) 4601–4612, https://doi.org/10.1002/adfm.201600590.

[16] M.H. Park, H.J. Kim, Y.J. Kim, Y.H. Lee, T. Moon, K.D. Kim, S.D. Hyun, C.S. Hwang, Study on the size effect in $Hf_{0.5}Zr_{0.5}O_2$ films thinner than 8 nm before and after wake-up field cycling, Appl. Phys. Lett. 107 (2015) 192907, , https://doi.org/10.1063/1.4935588.

[17] E.D. Grimley, T. Schenk, X. Sang, M. Pešić, U. Schroeder, T. Mikolajick, J.M. LeBeau, Structural changes underlying field-cycling phenomena in ferroelectric HfO_2 thin films, Adv. Electron. Mater 2 (2016) 1600173, , https://doi.org/10.1002/aelm.201600173.

[18] M.H. Park, T. Schenk, C.M. Fancher, E.D. Grimley, C. Zhou, C. Richter, J.M. LeBeau, J.L. Jones, T. Mikolajick, U. Schroeder, A comprehensive study on the structural evolution of HfO_2 thin films doped with various dopants, J. Mater. Chem. C 5 (2017) 4677–4690, https://doi.org/10.1039/C7TC01200D.

[19] M. Avrami, Kinetics of phase change. I general theory, J. Chem. Phys. 7 (1939) 1103–1112, https://doi.org/10.1063/1.1750380.

[20] T.Y. Lee, K. Lee, H.H. Lim, M.S. Song, S.M. Yang, H.K. Yoo, D.I. Suh, Z. Zhu, A. Yoon, M.R. MacDonald, X. Lei, H.Y. Jeong, D. Lee, K. Park, J. Park, S.C. Chae, Ferroelectric polarization-switching dynamics and wake-up effect in Si-doped HfO_2, ACS Appl. Mater. Interfaces 11 (2019) 3142–3149, https://doi.org/10.1021/acsami.8b11681.

[21] A.K. Tagantsev, M. Landivar, E. Colla, N. Setter, Identification of passive layer in ferroelectric thin films from their switching parameters, J. Appl. Phys. 78 (1995) 2623–2630, https://doi.org/10.1063/1.360122.

[22] M.H. Park, H.J. Kim, Y.J. Kim, Y.H. Lee, T. Moon, K.D. Kim, S.D. Hyun, F. Fengler, U. Schroeder, C.S. Hwang, Effect of Zr content on the wake-up effect in $Hf_{1-x}Zr_xO_2$ films, ACS Appl. Mater. Interfaces 8 (2016) 15466–15475, https://doi.org/10.1021/acsami.6b03586.

[23] R. Materlik, C. Künneth, A. Kersch, The origin of ferroelectricity in $Hf_{1-x}Zr_xO_2$: a computational investigation and a surface energy model, J. Appl. Phys. 117 (2015) 134109, , https://doi.org/10.1063/1.4916707.

[24] E.D. Grimley, T. Schenk, X. Sang, M. Pešić, U. Schroeder, T. Mikolajick, J.M. LeBeau, Structural changes underlying field-cycling phenomena in ferroelectric HfO_2 thin films, Adv. Electron. Mater. 2 (2016) 1600173, , https://doi.org/10.1002/aelm.201600173.

[25] Y. Ishibashi, H. Orihara, A theory of D-E hysteresis loop - application of Avrami model, Integrated Ferroelectrics Int. J. 9 (1995) 57–61, https://doi.org/10.1080/10584589508012906.

[26] S.M. Yang, J.Y. Jo, T.H. Kim, J.G. Yoon, T.K. Song, H.N. Lee, Z. Marton, S. Park, Y. Jo, T.W. Noh, Ac dynamics of ferroelectric domains from an investigation of the frequency dependence of hysteresis loops, Phys. Rev. B 82 (2010) 174125, , https://doi.org/10.1103/PhysRevB.82.174125.

[27] R.B. Iverson, R. Reif, Recrystallization of amorphized polycrystalline silicon films on SiO_2: temperature dependence of the crystallization parameters, J. Appl. Phys. 62 (1987) 1675, https://doi.org/10.1063/1.339591.

[28] T. Klemmer, D. Hoydick, H. Okumura, B. Zhang, W.A. Soffa, Magnetic hardening and coercivity mechanisms in L10 ordered FePd ferromagnets, Scripta Metall. Mater. 33 (1995) 1793–1805, https://doi.org/10.1016/0956-716X(95)00413-P.

[29] M.I. Morozov, D. Damjanovic, Hardening-softening transition in Fe-doped Pb(Zr,Ti)O_3 ceramics and evolution of the third harmonic of the polarization response, J. Appl. Phys. 104 (2008) 034107, , https://doi.org/10.1063/1.2963704.

[30] B. Traoré, K. Xue, E. Vianello, G. Molas, P. Blaise, B.D. Salvo, A. Padovani, O. Pirrotta, L. Larcher, L.R.C. Fonseca, Y. Nishi, Investigation of the role of electrodes on the retention performance of HfO_xbased RRAM cells by experiments, atomistic simulations and device physical modeling, IEEE International Reliability Physics Symposium (IRPS), IEEE Trans. Electron Devices, 2013, , https://doi.org/10.1109/IRPS.2013.6532041 2013, pp. 5E.2.1-5E.2.6.

[31] F.P.G. Fengler, M. Pešić, S. Starschich, T. Schneller, C. Künneth, U. Böttger, H. Mulaosmanovic, T. Schenk, M.H. Park, R. Nigon, P. Muralt, T. Mikolajick, U. Schroeder, Domain pinning: comparison of hafnia and PZT based ferroelectrics, Adv. Electron. Mater. 3 (2017) 1600505, , https://doi.org/10.1002/aelm.201600505.

[32] P. Marton, C. Elsässer, Switching of a substitutional-iron/oxygen-vacancy defect complex in ferroelectric $PbTiO_3$ from first principles, Phys. Rev. B 83 (2011) 020106, , https://doi.org/10.1103/PhysRevB.83.020106.

[33] C.H. Park, D.J. Chadi, Microscopic study of oxygen-vacancy defects in ferroelectric perovskites, Phys. Rev. B 57 (1998) R13961, , https://doi.org/10.1103/PhysRevB.57.R13961.

[34] R. Materlik, C. Künneth, A. Kersch, The origin of ferroelectricity in $Hf_{1-x}Zr_xO_2$: a computational investigation and a surface energy model, Appl. Phys. Lett. 117 (2015) 134109, , https://doi.org/10.1063/1.4916707.